Behavior of steps on Si(001) as a function of vicinality

B. S. Swartzentruber, N. Kitamura, M. G. Lagally, and M. B. Webb
University of Wisconsin–Madison, Madison, Wisconsin 53703
(Received 17 March 1992)

The surface step morphology of the Si(001) surface as a function of miscut angle between 0.3° and 5.25° has been investigated using scanning tunneling microscopy. On samples with large average terrace widths, the kinks in the steps behave independently and the intrinsic step energy can be determined from the kink-length distribution which follows simple Boltzmann statistics. For wide terraces the large-scale meandering of the steps is governed by the long-range strain fields caused by the anisotropic surface stress tensor. Here the step separation distributions can be described by a Boltzmann distribution of segments of the step moving in this strain potential. At intermediate average terrace widths, the distribution of kink lengths is influenced by the confinement between neighboring steps, which suppresses the number of long kinks. As steps get closer together, a short-range direct step-step interaction arising from the local strain due to the rebonding of the SB step begins to influence the step distribution. The sense of this interaction is such that the rough SB step is attracted to its downhill neighbor. Images and terrace-width distributions of surfaces for which the miscut angle is great enough to measure an appreciable increase in the percentage of double atomic-height steps are used to provide a description of the evolution of the surface from one containing single-height to mostly double-height steps.

I. INTRODUCTION

The scanning tunneling microscope allows direct observation of the morphology of surface steps and detailed measurements of the statistical distributions of separations between steps or terrace widths, of the separations between kinks along a step, and of the lengths of the kinks. From these distributions it is possible to determine the step contributions to the surface free energy. There are potentially many such contributions which include (i) the intrinsic energy per unit length to form steps, (ii) the energy to form a kink in a step, (iii) interactions between kinks along a step, and (iv) interactions between steps. In turn, the step-step interactions can arise from (i) long-range strain fields in the substrate due to the intrinsic surface stress, (ii) an entropic effective interaction due to the confinement of a step between its neighbors, and (iii) direct interactions due to the details of the atomic and electronic structure of the steps.

In this paper we report measurements of these contributions for the Si(100) surface. In order to disentangle the many effects, we use a series of vicinal surfaces because the relative importance of the several contributions changes with different miscut angle, i.e., with average terrace width. Our objective is to determine the simplest model Hamiltonian that can reproduce the measured distributions.

The silicon (001) surface has been the subject of intense investigation both theoretically and experimentally. Not only is silicon technologically important, but it displays a rich variety of surface phenomena that make it an interesting model system. The silicon (001) surface reconstructs to form rows of dimerized atoms giving a (2×1) reconstruction (Fig. 1). Because of the diamond-lattice structure, the dimer direction is orthogonal on terraces separated by an odd number of single-height steps, giving rise to both (2×1) and (1×2) domains. On surfaces with only single-height steps, terraces can be terminated by two types of step. Following the convention of Chadi, step segments on which the upper-terrace-dimerization

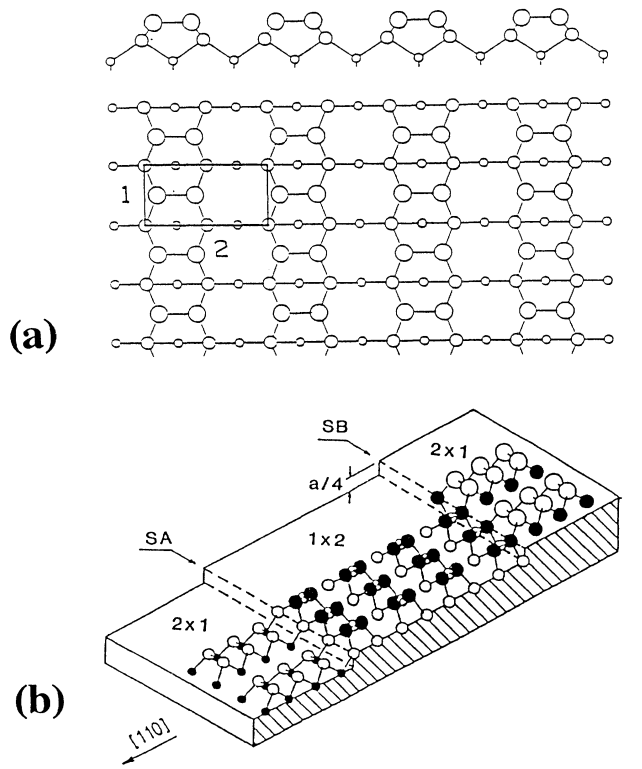

FIG. 1. Ball-and-stick model of the Si(001) surface. The surface reconstructs to form rows of dimerized atoms. Dimer rows are orthogonal on terraces separated by an odd number of single steps. The two types of steps SA and SB are indicated.

direction is perpendicular (parallel) to the step are called SA (SB).[1] On surfaces that are miscut towards a [110] direction, the two types of steps alternate. Steps that run nominally parallel to the upper-terrace dimer-bond direction contain many kinks and are rough, whereas steps that run nominally perpendicular to the upper-terrace dimer-bond direction contain few kinks and are smooth. Kinks in the rough (nominally SB) step are comprised of segments of SA termination and kinks in the smooth (nominally SA) step are comprised of segments of SB termination. We will use the words "rough" and "smooth" to refer to the two types of steps as a whole, and reserve the terms "SB" and "SA" to refer to the microscopic termination of a step segment. Terraces on the upper side of the rough steps we call (2×1) and terraces on the upper side of the smooth steps we call (1×2). (Surfaces that are miscut towards a [100] direction are comprised of steps that run nominally at 45° to the dimers, and in this case all of the steps are equivalent.)

In this introduction we first need to briefly review earlier work, done primarily on wide terraces, and then we discuss additional effects expected for larger miscut angles. First, it was recently observed in low-energy-electron-diffraction (LEED) measurements that the relative surface domain populations are affected by the application of an externally applied uniaxial stress;[2] under applied stress, one domain grows at the expense of the other. The domain with its dimer bond compressed is favored. Subsequent scanning-tunneling-microscopy (STM) measurements[3] determined that the surface remains a striped phase under external stress, i.e., striped terraces separated by monatomic steps. Steps are not created nor do they bunch together to form facets; the average distance between like steps remains that which is determined by the miscut angle and is independent of the applied stress.

These LEED and STM observations were explained within continuum elastic theory by Alerhand *et al.*[4] The silicon (001) intrinsic surface stress tensor is anisotropic with the surface in tension along the direction parallel to the dimer bond and in compression perpendicular to the dimer bond. Because of the discontinuity in the surface stress at the domain boundaries, there are force monopoles at each step that produce strain fields that extend into the bulk, and the steps arrange themselves to minimize the energy in these long-range strain fields. These authors considered a striped phase with straight walls. Under external stress the elastic energy per unit step length is given by[5]

$$E_{\rm el}(p)=\lambda_{\rm SA}+\lambda_{\rm SB}+2a_0plF\epsilon-2\lambda_\sigma\ln\left[\frac{1}{\pi a}\cos\frac{\pi p}{2}\right]. \quad (1)$$

Here the displacement of a step from the midpoint between its neighbors is pl, where l is the average terrace width measured in units of dimer spacings $(2a_0)$; the average widths of the majority and minority domains are $(1+p)l$ and $(1-p)l$; ϵ is the strain due to the external stress; $F=\sigma_{\parallel}-\sigma_{\perp}$ is the anisotropy of the intrinsic surface stress tensor; and $\lambda_{\rm SA}$ and $\lambda_{\rm SB}$ are the intrinsic step creation energies per unit length. λ_σ contains F and bulk elastic constants: $\lambda_\sigma=F^2(1-\nu)/2\pi\mu$. a is a microscopic cutoff length (in units of $2a_0$) of the order of an interatomic spacing, i.e., $a\sim\frac{1}{2}$. The optimum p is determined by minimizing this energy, giving

$$p_0=\frac{2}{\pi}\tan^{-1}\left[\frac{2a_0lF\epsilon}{\pi\lambda_\sigma}\right]. \quad (2)$$

Thus, a step can be viewed as sitting in a potential, between its neighbors, due to the long-range strain fields arising from the anisotropic stress tensor. We call this the "Alerhand energy."

In a second previous work, STM images of vicinal Si(001) were analyzed to determine the distribution of kink separations and kink lengths from which step and kink energies can be directly determined.[6] (On the rough step, "kink separations" are defined as the lengths of the SB-terminated segments and "kink lengths" are defined as the lengths of the SA-terminated segments.) It was found that, on surfaces with sufficiently large average terrace widths, kinks exhibit independent behavior, and that the kink-length distribution follows simple Boltzmann statistics. By "independent," we mean that the probability of a kink occurring at any potential kink site does not depend on the neighboring configuration. The probability of two kinks separated by s units is equal to the probability of not having a kink for $s-1$ consecutive units, multiplied by the probability of having a kink, $P(s)=(1-P_k)^{s-1}P_k$,[7] where P_k is the probability of having a kink of any length or either direction. The probability of measuring a kink of length n is proportional to $\exp[-E(n)/kT]$. From the measured kink-length distribution, the result is that $E(n)=n\lambda_S+\lambda_C$, which is most naturally interpreted as the sum of a step creation energy per unit length λ_S, and a constant, independent of kink length, most simply attributed to a "corner" energy.[8]

Finally, again from STM measurements on samples with wide terraces, it was demonstrated that the step separation distribution could be interpreted as step segments of some length ξ whose average positions populate the Alerhand potential with a simple Boltzmann distribution.[9] The parameter ξ scaled with the average terrace width.

The above analyses were based on the fact that the steps were widely spaced. For narrower terraces a number of additional effects become important.

First, the meandering steps are confined to meander only between their neighbors. This boundary condition imposes limitations on the possible step and kink configurations. It gives an entropic effective step-step interaction that is repulsive, both narrowing the terrace-width distributions and suppressing long kinks. Even if the kinks are energetically noninteracting, they can no longer be considered statistically independent. For the wide terraces discussed above it is the Boltzmann factor rather than the confinement that limits kink lengths and step meandering.

Second, the continuum elastic treatment of Alerhand *et al.*[4] neglected the possibility of any direct step-step interaction. Such an interaction has been predicted for

steps on the Si(001) surface due to the local strain field of the rebonded SB step interacting with the long-range strain fields.[10,11] For widely separated steps, neglecting this direct interaction is unimportant because it will typically fall off quickly with step separation; however, as the steps get closer together (with increasing sample miscut), the effect of any direct step-step interaction will become important.

Finally, there is the binding of two monatomic steps to form double-atomic-height steps. As the average terrace width decreases, the percentage of double steps increases; the double steps formed are always those that are parallel to the upper-terrace dimers, and are called the DB step.[12] The nature of the formation of the double steps has been the subject of considerably recent interest. The statistical mechanics of the surface for narrow terraces are, of course, greatly affected by the inclusion of the double steps in the problem.

To analyze the surface morphology for intermediate miscut angles, where the confinement of steps between their neighbors and the direct step-step interactions are important but where the presence of double steps can be neglected, one might use a model Hamiltonian that describes a rough step meandering between two straight steps,

$$H=\sum_i \lambda_{\mathrm{SA}}+\lambda_{\mathrm{SB}}+\lambda_{\mathrm{SA}}|h_i-h_{i+1}|+\lambda_C(1-\delta_{h_i,h_{i+1}}) -2\lambda_\sigma \ln\left[\frac{l}{\pi a}\cos\frac{\pi h_i}{2l}\right]+\lambda_d\left[\frac{a}{2l}\right]^2 -\sqrt{3\lambda_\sigma\lambda_d}\,\frac{a}{l}\tan\frac{\pi h_i}{2l}\ , \tag{3}$$

where h_i is the displacement in dimer units of the lth column from the midpoint between neighboring steps. λ_σ and λ_d are force monopole and force dipole elastic coefficients arising from the anisotropic surface stress tensor and from the rebonding of the SB steps, respectively. The third and fourth terms in the Hamiltonian are the kink energy including the "corner" energy. The fifth term is the Alerhand elastic energy, and the last two terms are the dipole-monopole direct step-step interaction. This Hamiltonian neglects any fluctuations in the SA steps and assumes they are straight walls.[13,14]

With this model Hamiltonian, the statistical mechanics of the system, e.g., the free energy and the statistical distributions, can be solved for exactly using the transfer-matrix formalism.[15] It is our object to see if this Hamiltonian is in fact sufficient to describe the experimental data and, if it is, to determine the parameters.

The paper is organized as follows. In the next section the experimental details are presented. Material is presented in the rest of the paper emphasizing the role of average step separation as a variable. The third section presents the statistical effect of the step confinement on the kink-length distribution as the average terrace width becomes narrower. The fourth section presents the step-separation distribution. It gives a comparison of the relative importance of the Alerhand strain potential and the entropy in determining the properties of the step-separation distribution on samples with a relatively large average terrace width. It also gives an analysis of the asymmetry in the domain populations as a function of miscut which gives a measure of the direct step-step interaction. The fifth section is a discussion of the parameters used in the fitting of the distributions. Last, in the sixth section we present various statistical distributions, characterizing the steps, for various miscut angles where the percentage of double steps becomes appreciable.

II. EXPERIMENT

All experiments are carried out in a stainless-steel ultrahigh-vacuum (UHV) chamber with a base pressure of less than 2×10^{-10} Torr. The chamber contains a home-made STM, a set of manipulators, two slotted storage racks for extra samples, and a manipulator for transferring samples between the various regions of the chamber.

The STM is wholly contained on an 8-in conflat flange, which mounts onto the side of the chamber. The STM is comprised of two Burleigh UHV-compatible inchworm motors[16] mounted on a copper base plate. One inchworm has the quadrant-tube scanner with a concentric tip mounted on its end, and serves to control the coarse Z motion or tip approach. The sample holder is mounted on the other inchworm, which can translate over a 20-mm range in increments of about 1 μm. The sample holder is comprised of two Ta blocks against which Ta foil springs hold the ends of the sample. By passing a current through the sample, it can be heated in the microscope while scanning. The chamber is mounted on pneumatic legs, the microscope hangs from springs, and there is eddy current damping.

The strainer-heating station utilizes two linear motion feedthroughs. One end of the sample bar $(25\times3\times0.5$ mm$)^3$ is clamped between two Ta plates using the first manipulator. Contact to the free end of the sample is made via a Ta anvil attached to the second manipulator.[9] This manipulator allows a variable external stress to be applied to the sample. Stress applied in this fashion leads to a surface strain that varies linearly along the sample from a maximum at the fixed end to zero at the free end. The sample is heated by passing a current through the sample, between the Ta contacts. It is important that this cantilevered mounting allows observations of samples with zero external stress, which is not necessarily the case in arrangements in which both ends of the sample are rigidly clamped. A central manipulator is used to transfer up to six samples between the microscope, the heating station, and the parking lot and junk yard.

Sample temperatures above 675 K are measured using an IR pyrometer and a disappearing-filament pyrometer. For measuring lower temperatures, a W-5% Re/W-26% Re thermocouple is attached separately to the central manipulator so it can be pressed against the back side of the samples in either the microscope or heating station. To avoid contamination, the thermocouple never touches samples from which data are to be taken; the thermocouple is used only after the measurements are completed.

The measurements reported in this study were taken from 0.5-mm-thick highly doped Si wafers with a variety of miscut angles about the (001) direction (from 0.3° to 5.25° towards [110]).[17] The wafers are cut with a diamond saw to give $25\times3\text{mm}^2$ samples. In UHV the samples are cleaned using a recipe described before.[18] Briefly, the samples are heated to 1525 K for 30 sec several times and then annealed at 875 K for 5 min and radiation quenched. This cleaning procedure can yield surfaces with as little as 0.5% surface defect density. This is sufficiently small that the defects do not influence the statistical analyses to be presented. In any case there is no apparent correlation, such as pinning, between the step structure and the most common defects. It should be noted that the first sample used after closing the chamber, although prepared identically, serves to outgas and clean the heating station and may have several percent more defects than subsequent samples. This first sample is discarded.

The STM feedback electronics are operated in constant current mode with a typical bias voltage between 1.5 and 3.0 V, with the tip positive with respect to the sample, and tunneling currents of between 0.05 and 1.0 nA. The STM is controlled by a computer running SHOESCAN-STM acquisition and control software.[19] In these experiments, the images contain 512×512 pixels with 256 colors and cover scan ranges between 600 ad 1200 Å (~5 pixels/dimer spacing). The scan rotation angle is chosen so that the scanning direction is 45° to the dimer rows. This insures that both the (1×2) and (2×1) domains are visible when the image is displayed in derivative mode. A typical image is displayed in Fig. 2. To get reasonable statistics, each data set consists of a number of images. The total length of each type of step in every data set is greater than 5000 dimer units. The number of images required to complete a data set depends on the vicinality, or average step separation, and varies from four images on the 5.25° samples to 15 on the 0.3° samples. After taking a complete set of images, the position of every step in each image is then digitized. The thermodynamic distributions are measured from these digitized images.

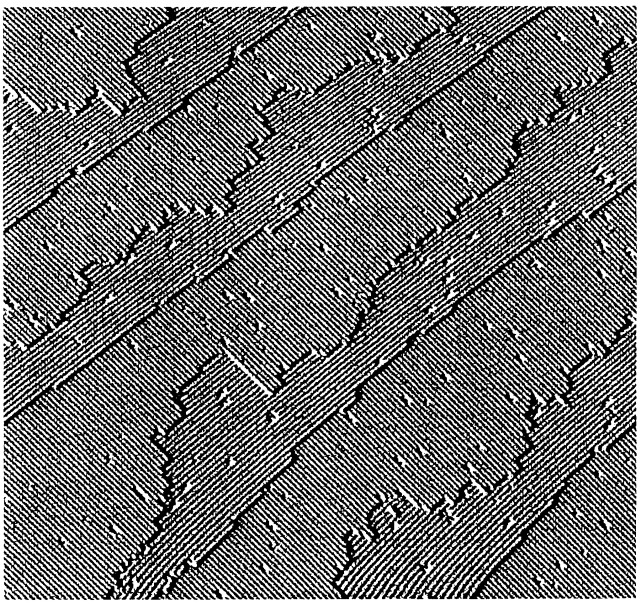

FIG. 2. STM images of a 0.5° miscut Si(001) surface displayed in derivative mode. From left to right, areas that slope up are displayed as white and areas that slope down are displayed as black. The surface steps down from upper left to lower right. The alternating domains and the two types of steps (rough and smooth) can easily be seen.

All of the samples used to acquire data from which the thermodynamic distributions are measured are prepared identically. After the standard initial cleaning procedure described above, the samples are annealed at 875 K for 5 min and then radiation quenched to room temperature by disconnecting the heating current. The samples are then taken from the heating station with the manipulator and placed in the microscope. Because of the small thermal mass of the samples, the thermal drift is small enough, i.e., <1 Å/sec, that images can be obtained within 15 min after the sample was at 1525 K in the heating station. This short-time constant is a major advantage of transporting the samples by themselves, as opposed to clamping the samples in a movable sample holder that also heats up during sample preparation.

III. KINK LENGTH DISTRIBUTION

The earlier analysis of the kink-length distributions from samples with wide terraces depended upon the kinks being statistically independent so that the probability of a kink of a given length was given by the Boltzmann factor for its energy. In fact, the steps are confined to move only between their neighbors. When a step is located close to a neighboring step, the choice of kink lengths is restricted because steps cannot cross. This restriction tends to suppress the number of long kinks close to a neighboring step. This "end effect" becomes increasingly important as the average terrace width gets small. In this section we will address what effect his confinement has on the distribution of kink lengths.

To observe the effect of the confinement, we have measured the kink-length distribution as a function of the average terrace width. In Fig. 3 we show a plot of the probability $P(n)$ of having kinks of length n versus n for different average terrace widths. The symbols represent the measured values. Within the experimental error, the data from samples with terrace widths ≥150 Å (miscut angles $\leq0.5°$) lie on top of one another. We observe, however, that long kinks become less likely on samples with terraces ≤80 Å (miscut angles $\geq1.0°$).

The solid lines in Fig. 3 are the result of transfer-matrix calculations of $P(n)$ for various miscut angles using the full Hamiltonian of Eq. (3) and values of the parameters listed in the caption. (We return later to a discussion of these values.) The dashed line is the Boltzmann distribution of kink lengths whose energies are $n\lambda_{SA}+\lambda_C$; it is also the limiting result of the transfer-matrix calculation as the average terrace width gets arbitrarily large.

We conclude that, for terrace widths ≥150 Å, the

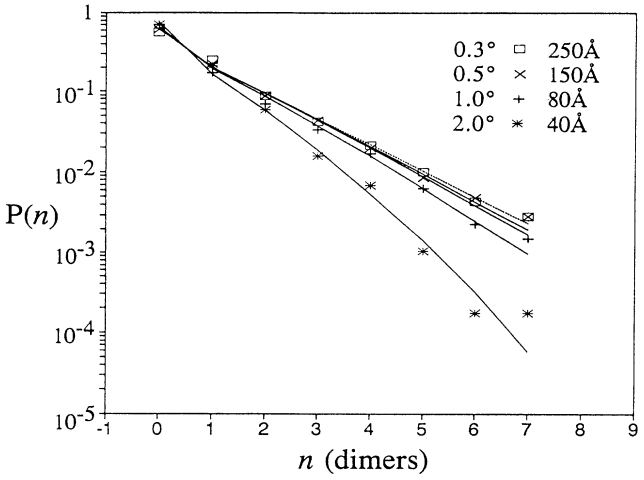

FIG. 3. Probability of a kink of length $\pm n$ atoms vs n for four values of the average step separation showing the suppression of long kinks as the terrace width decreases. The measured data for the rough steps are plotted as symbols and the calculations are plotted as lines.

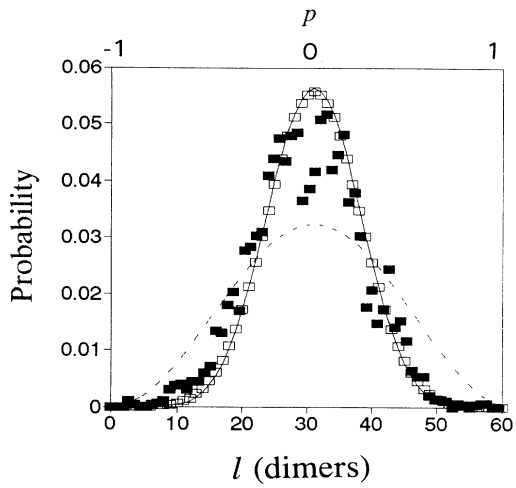

FIG. 4. Measured step-separation distribution for a 0.3° miscut sample. The data are displayed as the closed squares. The open squares are the transfer-matrix calculation. The solid line is a Boltzmann distribution in the Alerhand potential and the dashed line is the cosine-squared function, which is the low-temperature distribution in a square well.

kinks indeed exhibit independent behavior, and the slope of the kink-length distribution is determined by the Boltzmann factor of the kink energy as assumed in the earlier analysis. That is, for wide terraces it is primarily the energy of the long kinks that makes them unfavorable rather than the presence of the neighboring steps.

IV. STEP-SEPARATION DISTRIBUTION

The step-separation distributions give a measure of the step-step interactions. On wide terraces, the dominant interactions are effective, indirect step-step interactions, such as the effective entropic repulsion due to the confinement of steps between their neighbors or, for the specific case of Si(001), due to the long-range strain fields, i.e., the Alerhand energy. For narrower terraces, "direct" interactions due to the detailed structure of the steps will be important. We begin by considering the distributions for wide terraces. An example of a measured terrace width distribution for an average terrace width of 250 Å (miscut angle $=0.3°$) is shown as the closed squares in Fig. 4.

Earlier it was recognized that for sufficiently wide average terrace widths, the step-separation distributions could be described as a Boltzmann distribution of segments of a step of length ξ whose average position moved in the Alerhand potential. Further, the parameter ξ was found to be proportional to the average terrace width $\langle l \rangle$.[9]

For this simplest model, the distribution $P(p)$ is

$$P(p) \alpha \exp\left[-\frac{\xi E_{\rm el}(p)}{kT}\right] \alpha \left[\cos\frac{\pi p}{2}\right]^{\kappa}, \tag{4}$$

where

$$\xi E_{\rm el}(p) = -2\lambda_0 \xi \ln\left[\cos\frac{\pi p}{2}\right] \tag{5}$$

is the energy of a step segment of length ξ in the Alerhand potential from Eq. (3), and

$$K = \frac{2\lambda_0 \xi}{kT} . \tag{6}$$

This probability $P(p)$ is plotted as the solid line in Fig. 4 using a value for $K=6.14$. For our parameters, this fit gives $\xi = 0.2l$. This is to be contrasted with

$$P(p) \alpha \left[\cos\frac{\pi p}{2}\right]^2 , \tag{7}$$

which is the low-temperature result for a wall confined between its neighbors but with no Alerhand potential, i.e., moving in a square well.[20] This probability is plotted as the dashed line in Fig. 4.

This simple picture of a Boltzmann distribution of terrace widths can be justified by coarse graining the transfer matrix. The idea is to calculate the statistical mechanics for step segments of finite length M to determine the smallest segment that reproduces the results of the exact theory in the thermodynamic, or infinite-length, limit. Figure 5(a) is a plot of the diagonal elements $T^M(ii)$ of the Mth power of the transfer matrix versus i for increasing powers M. These are the terrace-width distributions for segments of length M, with periodic boundaries. The innermost curve is the exact result in the thermodynamic limit. We do this for various miscut angles, and in Fig. 5(b) we plot the length of the segment M, beyond which the diagonal elements come within $\delta = 1\%$ of the exact result, as a function of terrace width.

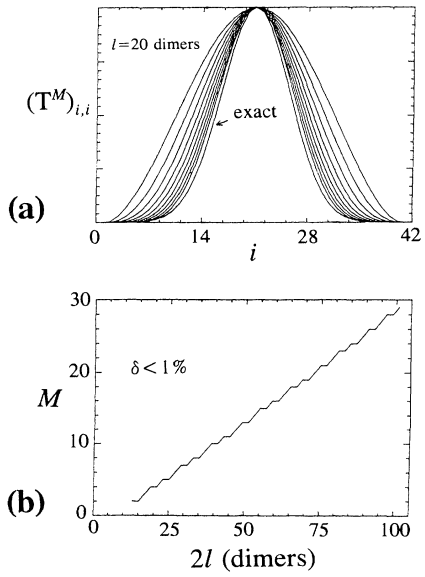

FIG. 5. (a) Plots of the diagonal elements of the Mth power of the transfer matrix for increasing M. The diagonal elements are the step-separation distributions for step segments of length M. The exact solution, i.e., the thermodynamic limit, is the innermost curve. (b) Number of iterations M required to come within 1% of the exact solution as a function of terrace size. M scales linearly with l, slope ~ 0.7.

This length, which is associated with ξ, is seen to be directly proportional to the terrace width. In this case $\xi/l=0.7$, but this ratio depends somewhat on the value chosen for δ.

The diagonal elements of the coarse-grained transfer matrix are shown as the open rectangles in Fig. 4; they are indeed essentially the Boltzmann factors of a rescaled Alerhand energy with weight ξ. Thus we have regained the simple picture of segments of the step moving independently in the Alerhand potential.

An important observation in the measured step-separation distributions is that the exponent of the cosine K scales with l, whereas the distribution in the square well, $\cos^2$, does not. This result clearly illustrates the importance of the Alerhand potential, compared to purely entropic considerations, in determining the step-separation distribution on samples with wide average terrace widths.

We now discuss step-separation distributions for intermediate average terrace widths, where the effect of the "direct" step-step interaction is evident but where the amount of double steps is unimportant. Previous electron-diffraction experiments have shown a domain population asymmetry for vicinalities where one would not expect the presence of double steps to be significant.[21–23] Indeed, our STM measurements confirm that for average terrace widths greater than ~ 65 Å (miscut angles $\leq 1.2°$) the surface is comprised of less than 2% double steps.

In addition to a force monopole treated by Alerhand *et al.*, a step may also include higher-order multipoles. In particular, Marchenko pointed out the possibility of two types of force dipoles occurring at steps,[24] one with a nonzero net moment, $\uparrow\downarrow$, and another with no moment, $\leftarrow\rightarrow$, which we will call a z dipole and an x dipole, respectively. The z dipole exerts a torque that tends to twist the surface, whereas the x dipole tends to stretch the surface. The magnitude of these terms is governed by the local strain at the steps due to the details of the surface reconstruction and atomic arrangement of the steps. For the Si(001) surface, calculations have predicted that local strain at the steps will give rise to appreciable force dipole terms only for the rebonded SB steps.[1,10]

The force dipole of an SB step can interact with the force monopole of its neighboring SA steps.[10,11] The monopole has a force only in the plane of the surface, i.e., in the x direction. Only the x dipole can couple to the monopole, which gives rise to an interaction energy that scales like $1/l$. The energy per unit step length can be calculated analytically for straight steps and is asymmetric with respect to displacement of the SB step from the midpoint between its neighboring SA steps, $E_{\text{dipole}}(p) \propto \tan(\pi p/2)$.[11] The sense of the asymmetry is such that the rough step is attracted to its downhill neighbor, favoring (2×1) domains. Without including higher-order interactions, the total p-dependent part of the energy, for a step pair, is simply the sum of the monopole-monopole, i.e., Alerhand, and dipole-monopole terms, and is given by

$$E(p)=\lambda_0-2\lambda_\sigma \ln\left[\cos\frac{\pi p}{2}\right]-\sqrt{3\lambda_\sigma\lambda_d}\,\frac{a}{l}\tan\frac{\pi p}{2}\,. \qquad (8)$$

This is identical to Eq. (3); except for simplicity, all of the non-p-dependent terms have been lumped into the constant λ_0. In Fig. 6, we have plotted this energy for several values of the coefficient of the tangent term. The minimum in the energy is located at

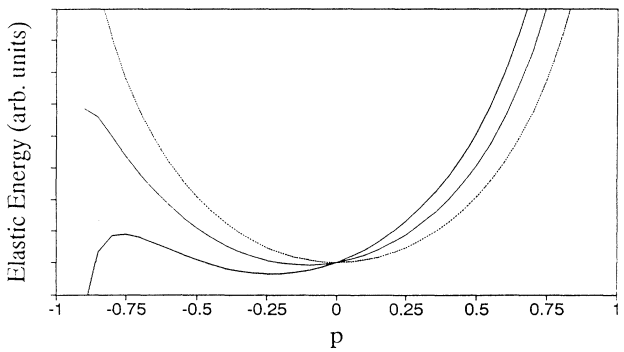

FIG. 6. Plot of the calculated continuum elastic potential energy as a function of the displacement of a step from the midpoint between its neighbors for three values of the average step separation. The energy contains both the strain energy in the long-range strain fields due to the anisotropic surface stress tensor and the direct step-step interaction energy arising from the local strain of the rebonded SB step.

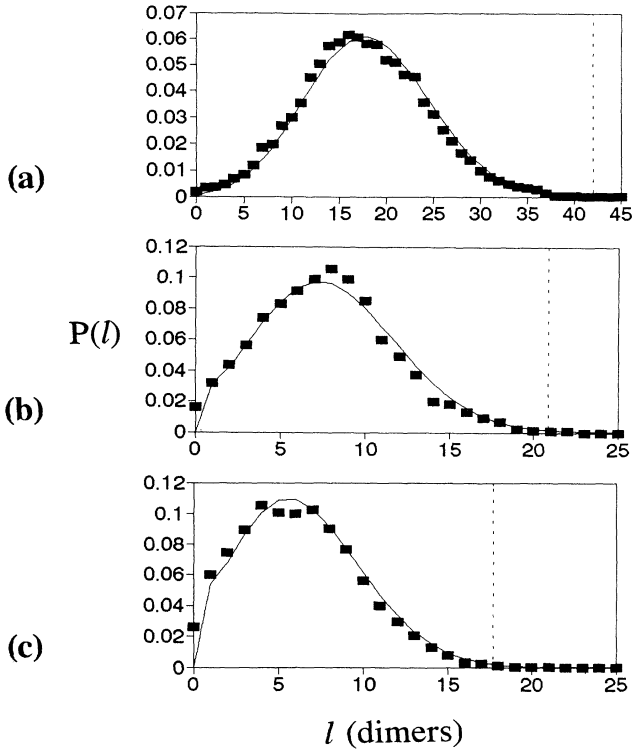

FIG. 7. Measured (closed squares) and calculated (solid line) terrace-width distributions for the (1×2) domain for samples with intermediate average step separations, (a) 150 Å (0.5°), (b) 80 Å (0.9°), and (c) 67 Å (1.1°). The calculated curves are fit to the data using transfer-matrix methods and the Hamiltonian of Eq. (3), using the ratio of λ_d to λ_σ as an adjustable parameter. The dashed line is the best-fit continuum elastic potential (arb. units) for each data set.

$$p_0=\frac{1}{\pi}\sin^{-1}\left[\sqrt{3\lambda_d/\lambda_\sigma}\,\frac{a}{l}\right]. \tag{9}$$

Thus, the optimum p increases monotonically as the average terrace width decreases. There is no local minimum for average terrace widths small enough that the argument of the inverse sine is greater than 1.

We have a direct measure of the strength of the dipole-monopole interaction by fitting the step-separation distributions for average step separations greater than 65 Å. At these vicinalities the average step separation is great enough that continuum elasticity should be appropriate and the situation is not complicated by the presence of double steps. Figure 7 shows the (1×2) terrace-width distribution data, displayed as closed squares, for samples with average terrace separations of 150, 80, and 67 Å. We have calculated distributions using the transfer matrix incorporating the Hamiltonian of Eq. (3), treating the ratio of λ_d to λ_σ as an adjustable parameter. The transfer-matrix results are displayed as the solid lines in Fig. 7. Best fits to the data are obtained with $\lambda_d/\lambda_\sigma=125$.

V. PARAMETERS

We now discuss the fitting and parameters in more detail. We set out to ask if the model Hamiltonian of Eq. (3) is sufficient to describe the steps on the Si(001) surface. This Hamiltonian includes the step and corner creation energies with the parameters λ_{SA}, λ_{SB}, and λ_C, the Alerhand long-range strain field energy involving λ_σ, and the direct step-step interaction involving λ_d. The data consist of (i) the earlier measurements by Men of the domain populations p_0 as a function of external strain; (ii) $P(n)$, the kink-length distributions for quenched samples that are presumably characteristic of a king-length freeze-out temperature T_k; and (iii) $P(p)$, the step-separation distributions also for quenched samples that are characteristic of a generally different terrace-width freeze-out temperature T_p. All of these data are available for a range of vicinalities or average terrace widths.

All the comparisons of the transfer-matrix calculations to the data shown in Figs. 3, 4, and 7 have been made with the single set of parameters. The good fit indicates that the model Hamiltonian, using continuum elasticity theory with straight walls, is sufficient to describe the steps for wide and intermediate terrace widths for which double-height steps do not play a significant part. We now discuss the constraints on the fitting and the parameters.

The Hamiltonian as written is for rough steps meandering between fixed and equally spaced smooth neighbors. Actually, the smooth steps also meander slightly, leading to a distribution of SA-SA separations. For the present fits, we have used the transfer matrix to calculate the step-separation distributions for various SA-SA separations and then weighted these with the measured SA-SA distribution.

The terrace-width freeze-out temperature has been taken as $T_p=850$ K. We believe that the time constant for the terrace-width distribution to reach equilibrium, i.e., a process that involves atomic diffusion along the step, cannot be slower than the time constant for the steps to reach their steady-state configuration under the application of an external stress, i.e., a process that involves the formation and migration across the terraces of a diffusing species. Assuming a time constant fixed by the quench rate of 1 sec, measurements of the latter process[21] yield a freeze-out temperature of not more than 900 K, which puts the value of T_p near the upper allowable limit.

The values of the step and corner energies have been taken as $\lambda_{SA}=0.040$ eV/$(2a_0)$ and $\lambda_C=0.060$ eV. The analysis of the kink-length distributions[6] directly gave values of $\lambda_{SA}/kT_k=0.74(2a_0)^{-1}$ and $\lambda_C/kT_k=1.1$. The values chosen for the present fits then require that T_k be 625 K. It is reasonable that T_k be smaller than T_p since the kink distribution is a more "local" property. Preliminary high-temperature observations show that at 625 K there are appreciable local changes in the SB step configuration occurring on a time scale of tenths of sec.[25]

For these fits, the value of λ_σ has been taken as 4.9×10^{-3} eV/$(2a_0)$. Men's measurement of the domain populations as a function of external strain gave a measure of $F/\lambda_\sigma=49\pm7$ Å^{-1}. Our value of λ_σ would then

give $F=0.035$ eV/Å^2 using $F/\lambda_\sigma=56$ Å^{-1}. This gives for the value for the factor involving the bulk elastic constant $(1-\nu)/\pi\mu=1.0$ Å^3/eV, which is somewhat higher than the estimate used earlier.[26]

While each of the parameters required in the above discussion is perhaps reasonable, and while the simple model accounts for the essential features of the data, we know of a number of aspects of the problem which should be included more carefully. First, the elasticity problem has been done only for a strictly one-dimensional (1D) system, i.e., straight steps. There are indications that the elastic energy can be further reduced by allowing the steps to meander and solving the more complete 2D elastic surface problem.[27] Second, the SA as well as the SB steps meander, and the statistical mechanics should be done to account for the fluctuations in the SA-SA separations.[28] Finally, there is a binding of pairs of single steps into double steps. The experimental characterization of the evolution from single to double steps is discussed in the next section.

VI. DOUBLE STEPS

So far we have been discussing Si(001) surfaces with relatively small miscut angles. It is well known that Si(001) undergoes an evolution from a surface comprised of single-atomic-height steps to a surface comprised mostly of double-height steps as the miscut angle is increased. The details of this evolution have been a topic of recent interest both experimentally and theoretically. In this section we will present data measured for a variety of surfaces for which the miscut angle is great enough so that the surface contains an appreciable number of double steps. We present quantitative measurements of terrace-width distributions as a function of miscut in order to characterize the phenomenology of the evolution to double steps.

In Fig. 8 are displayed a set of images with miscut angles ranging from 1° to 5.25°. It is clear in these images that the percentage of the surface that is double stepped is increasing with miscut angle.

In Fig. 9 we present examples of measured (1×2) terrace width distribution $P(l)$ for several larger misorientations. The solid vertical line in each plot represents the measured average step repeat distance (SA-SA separation) for the particular miscut and delineates the average range over which the rough SB step can meander. The dashed vertical lines represent the mean minority terrace widths. The fraction of double steps is given by the value of $P(l)$ at l equal to zero dimers, and the mean of the distribution determines the relative domain populations.

Figure 10 is a plot of the fraction of double steps and of the relative area of the (1×2) domain as a function of miscut angle. These two quantities, although related, are essentially distinct characterizations of the evolution to double steps. At small miscut angles the relative domain size is changing due to the direct step-step interaction, whereas the percentage of double steps remains very small. In previous diffraction observations it was *only* the domain population asymmetry that was measured.

Neither the images of Fig. 8 nor the data in Fig. 10 in-

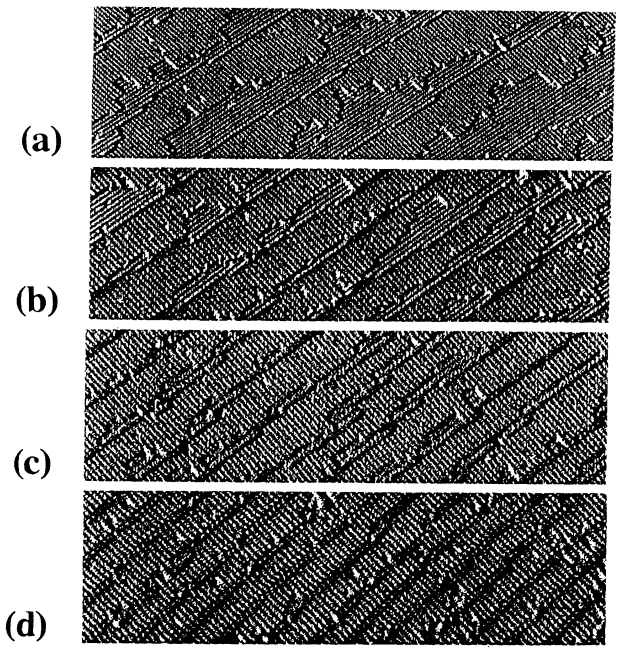

FIG. 8. STM images as a function of miscut angle. Horizontal scale is approximately 750 Å. Miscut angles: (a) 1°, (b) 2°, (c) 3°, and (d) 5°.

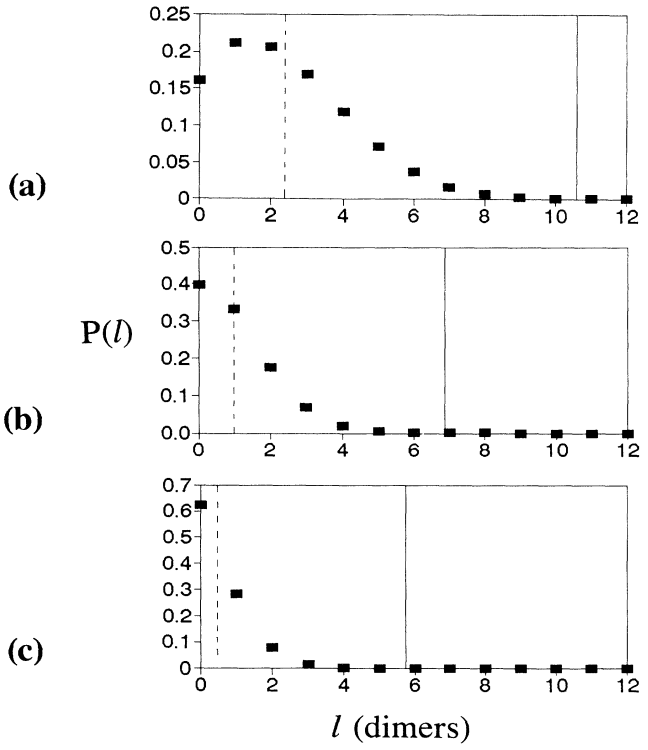

FIG. 9. Measured (1×2) terrace-width distributions from samples with (a) 2°, (b) 3°, and (c) 3.5° miscut angles. The vertical line is the average measured step repeat distance (SA-SA separation) in each data set.

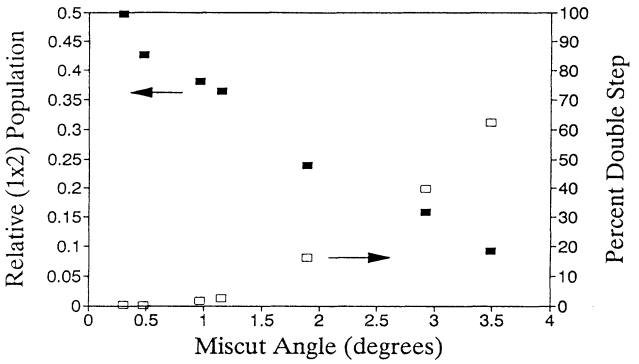

FIG. 10. Relative population of the (1×2) domain (closed squares, left axis) and percentage of double steps (open squares, right axis) measured from STM images as a function of miscut angle.

dicate that there is a distinct miscut where double steps begin to form. Also, there are not two distinct phases of double- and single-stepped regions. For these reasons we believe that it is inappropriate to consider this system as undergoing a phase transition as miscut is increased. It may be more useful to consider the system as a reaction, SA+SB$\rightleftarrows$DB; as the miscut increases, the increased step concentration drives the reaction to the right.

Fitting these distributions for the various vicinalities would be a critical test of any model describing the short-range step-step interaction and double-step (DB) binding energy. We note here that it is no longer appropriate to treat the system in the simple continuum elastic approximation used above for wider terraces because of the short length scale involved (only several atomic units); but, rather, atomistic calculations must be employed, e.g., Stillinger-Weber[10,11] or electronic total-energy calculations.

VII. CONCLUSIONS

We have examined the surface step morphology of the Si(001) surface as a function of miscut angles between 0.3 and 6°. On samples with large average terrace widths, the kinks behave independently and the kink-length distribution follows simple Boltzmann statistics. For sufficiently large average terrace widths, the large-scale meandering of the steps is governed by the long-range strain fields due to the anisotropic surface stress tensor. The terrace-width distributions can be described as a Boltzmann distribution of segments of the step moving together in the Alerhand strain potential.

As the terrace width decreases, the statistics of the kinks are influenced by the presence of neighboring steps, which suppresses the number of long kinks. For terrace widths greater than above 150 Å it is the energy of the long kinks that makes them unfavorable and not the presence of the neighboring steps. As steps get closer together, a short-range direct step-step interaction can be measured. This interaction is such that the rough step is attracted to its downhill neighbor and is due to the long-range Alerhand strain field interacting with the local strain arising from the rebonding of the SB step. Within the framework of transfer-matrix calculations and continuum elasticity theory, we can directly measure the strength of the dipole-monopole interaction.

Finally, we have presented images and terrace-width distributions of surfaces for which the miscut angle is great enough to measure an appreciable increase in the percentage of double steps. Along with the images of surfaces with large and intermediate average terrace widths, these images and distributions complete a description of the character of the evolution of the surface from single to mostly double steps.

ACKNOWLEDGMENTS

We would like to acknowledge many useful discussions with Bob Kariotis. This work was supported under NSF Grant No. DMR-9104437.

[1]J. D. Chadi, Phys. Rev. Lett. **59**, 1691 (1987).
[2]F. K. Men, W. E. Packard, and M. B. Webb, Phys. Rev. Lett. **61**, 2469 (1988).
[3]B. S. Swartzentruber, Y.-W. Mo, M. B. Webb, and M. G. Lagally, J. Vac. Sci. Technol. A **8**, 210 (1990).
[4]O. L. Alerhand, D. Vanderbilt, R. D. Meade, and J. D. Joannopoulos, Phys. Rev. Lett. **61**, 1973 (1988).
[5]This expression is different from that given in Ref. 4, Eq. (12), which is written in terms of energy per unit area. These two expressions are different by a factor of $2l$.
[6]B. S. Swartzentruber, Y.-W. Mo, R. Kariotis, M. G. Lagally, and M. B. Webb, Phys. Rev. Lett. **65**, 1913 (1990).
[7]Here we use kink separations measured in units of dimers ($2a_0$) rather than atoms (a_0). Therefore, the factor of $\frac{1}{2}$ does not appear in the exponent.
[8]H. J. W. Zandvliet, H. B. Elswijk, E. J. van Loenen, and D. Dijkkamp (unpublished). This work suggests that the corner energy might also be attributed to the energy of second-nearest-neighbor bonds. The dimers at corners have fewer second-nearest neighbors.
[9]M. B. Webb, F.-K. Men, B. S. Swartzentruber, R. Kariotis, and M. G. Lagally, Surf. Sci. **242**, 23 (1991).
[10]T. W. Poon, S. Yip, P. S. Ho, and F. F. Abraham, Phys. Rev. Lett. **65**, 2161 (1990).
[11]E. Pehlke and J. Tersoff, Phys. Rev. Lett. **67**, 465 (1991).
[12]J. E. Griffith and G. P. Kochanski, Solid State Mater. Sci. **16**, 255 (1990), and references cited therein.
[13]R. Kariotis (unpublished).
[14]J. Tersoff and E. Pehlke, Phys. Rev. Lett. **68**, 816 (1992).
[15]R. Kariotis and M. G. Lagally, Surf. Sci. **248**, 295 (1991).
[16]Burleigh Instruments, Burleigh Park, Fishers, NY 14453.
[17]Wacker-Chemitronic, D-8263 Burghausen, P.O. Box 1140, Germany.
[18]B. S. Swartzentruber, Y.-W. Mo, M. B. Webb, and M. G. Lagally, J. Vac. Sci. Technol. A **7**, 2901 (1989).
[19]SHOEMAKER STM, 4701 Pine St., Philadelphia, PA 19143.

[20]N. C. Bartelt, T. L. Einstein, and Ellen D. Williams, Surf. Sci. Lett. **240**, L591 (1990).
[21]M. B. Webb, F. K. Men, B. S. Swartzentruber, R. Kariotis, and M. G. Lagally, in *Kinetics and Ordering of Growth at Surfaces,* edited by M. G. Lagally (Plenum, New York, 1990).
[22]X. Tong and P. A. Bennett, Phys. Rev. Lett. **67**, 101 (1991).
[23]E. Schroeder-Bergen and W. Ranke, Surf. Sci. **259**, 323 (1991).
[24]V. I. Marchenko and A. Y. Parshin, Zh. Eksp. Teor. Fiz. **79**, 257 (1980) [Sov. Phys. JETP **52**, 129 (1980)].
[25]B. S. Swartzentruber, N. Kitamura, M. G. Lagally, and M. B. Webb (unpublished).
[26]D. Vanderbilt (private communication).
[27]M. B. Webb, F.-K. Men, and B. S. Swartzentruber, Bull. Am. Phys. Soc. **36**, 910 (1991).
[28]R. Kariotis (unpublished).